



The geochemistry and isotopic compositions of the Nakdong River, Korea: weathering and anthropogenic effects

Gyojin Keum · Yeongkyoo Kim ·
Kwang-Sik Lee · Jina Jeong

Received: 7 January 2022 / Accepted: 27 May 2022 / Published online: 8 June 2022
© The Author(s), under exclusive licence to Springer Nature Switzerland AG 2022

Abstract The Nakdong River is the longest river in South Korea, and flows through various geological terrains with different land use characteristics; therefore, the geochemistry of its water is expected to be influenced by many factors. In this work, the geochemical characteristics of the Nakdong River were examined, and its chemical compositions, δD , $\delta^{18}O$, and $\delta^{13}C_{DIC}$ values, and $^{87}Sr/^{86}Sr$ ratios were determined to investigate the geological and anthropogenic effects on the geochemistry of the Nakdong River water. The obtained concentrations of major ions were strongly affected by both the anthropogenic activity and weathering of the rocks. With increasing the flow distance, the ion concentrations slightly increased; and after the inflow of the Kumho River, which was the largest tributary running through Daegu (the fourth largest city in South Korea), the concentrations of Na and SO_4 ions abruptly increased and decreased again, suggesting the existence of strong anthropogenic effects caused by sewage treatment plants and dyeing industrial complex. Other activities such as agricultural ones also increased the NO_3 concentration. In July, the high precipitation level from tropical cyclones and downpours

decreased the ion concentrations as well as the δD and $\delta^{18}O$ values. The $\delta^{13}C_{DIC}$ magnitudes showed that the dissolved inorganic carbon mainly originated from mineral weathering upstream, while the oxidation of soil organic materials influenced by agricultural activity became more important downstream. The $^{87}Sr/^{86}Sr$ ratios revealed that in the upstream regions, the weathering of granite and gneiss complex was dominant, while in the downstream regions, the weathering of sedimentary rocks became more important. The weathering and anthropogenic effects on the river water chemistry were also demonstrated using statistical analysis, which revealed that the water geochemistry was mostly influenced by the anthropogenic sources, including industrial complex, represented by Na, Cl, and SO_4 . The obtained results show that, as compared to the geochemistry of the Han River (which is also a major river in Korea), the geochemistry of the Nakdong River is more influenced by anthropogenic activities (including agriculture and the industrial complex) due to the different land use.

Keywords Nakdong River · Hydrogeochemistry · Isotopes · Weathering · Anthropogenic effect · Pollution

G. Keum · Y. Kim (✉) · J. Jeong
School of Earth System Sciences, Kyungpook National
University, Daegu 41566, Republic of Korea
e-mail: ygkim@knu.ac.kr

K.-S. Lee
Korea Basic Science Institute, Daejeon 34133,
Republic of Korea

Introduction

The geochemistry of river water is influenced by many different factors. Weathering is one of such

factors caused by the water–rock interaction; therefore, this process plays an important role in the cycling of elements on the Earth surface (Lee et al., 2007; Balagizi et al., 2015). The chemical and isotopic composition of river waters provides useful information on the sources of major ions and chemical weathering rates of basins. Other processes such as evaporation, precipitation, and anthropogenic activity partially affect the geochemistry of river water (Kattan, 2015; Marchina et al., 2015; Wu et al., 2018). The anthropogenic activity becomes more important with the urbanisation of the drainage basin. However, the dissolution of carbonate and silicate minerals is the most important factor influencing the chemical compositions of major rivers in the world. The relationship between weathering and chemical compositions has been studied in detail for the Amazon, Ganges–Brahmaputra, Huanghe, Yangtze, Lena, and Mackenzie rivers (Gibbs, 1972; Stallard & Edmond, 1981, 1983, 1987; Sarin et al., 1989; Gordeev & Sidorov, 1993; Zhang et al., 1995; Huh et al., 1998a, b; Galy & France-Lanord, 1999; Chen et al., 2002; Bishwakarma et al., 2022). Recently, the isotopes of various elements were successfully applied to investigate the weathering process in the major rivers (Cai et al., 2020; Dellinger et al., 2021; Revels et al., 2021a, b).

Unlike major rivers elsewhere, the rivers in Korea are relatively short and are expected to be more severely affected by anthropogenic activities due to the high population density and various land uses, in addition to weathering. However, only the geochemical and isotopic compositions of the Han River, which is one of the major rivers in Korea and has a drainage basin of 26,018 km², have been extensively studied (Lee et al., 2007, 2008; Ryu et al., 2007). The obtained results showed that both parameters could be used as reliable indicators of the element origins and were strongly influenced by the rock types in the drainage basins (which can be classified into silicate and carbonate ones).

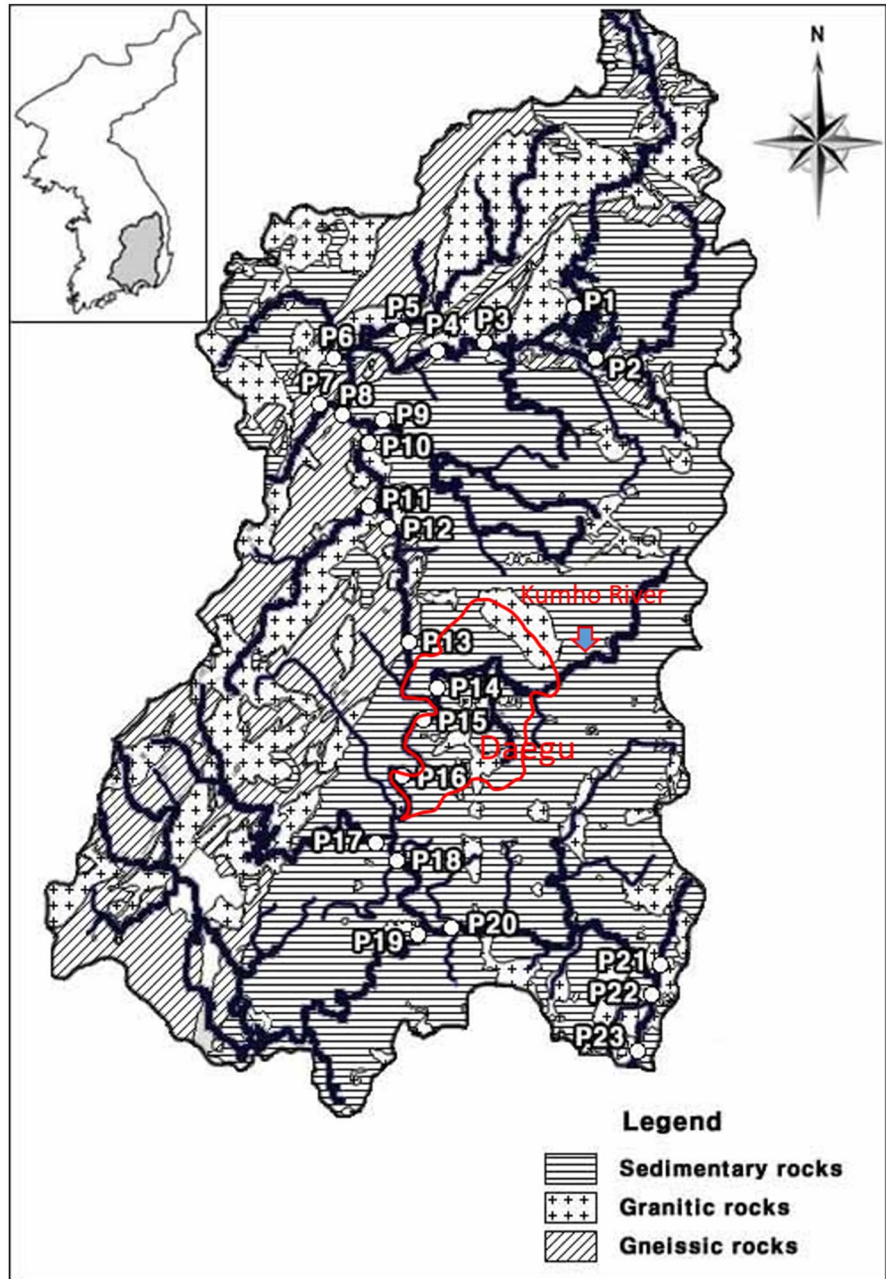
The Nakdong River is the second largest, but longest river in Korea (Fig. 1). Its length amounts to 506.17 km, and the drainage area of the Nakdong basin is 23,384.21 km². However, the geochemical and isotopic characteristics of the Nakdong River water have not been examined at all, although several water quality assessment studies involving

perchlorate, polychlorinated biphenyl, nitrate, phosphate, and other mutagenic chemicals were performed due to its importance as a public water supply source to the second and fourth largest cities in Korea (Busan, and Daegu, respectively) (Chop et al., 1999; Kim et al., 1998; Kwon et al., 2008; Quiñones et al., 2007).

The Nakdong River consists of several large tributaries. Its largest tributary is the Kumho River, which meets the mainstream of the Nakdong River at Daegu. Detailed geochemistry and isotope studies of the Kumho River were conducted previously (Kim & Kim, 2013). Their results indicate that the river water is strongly influenced by both weathering and the anthropogenic activity. In the upper regions of the Kumho River, the weathering of volcanic rock is the dominant process affecting the geochemistry of its water, while in the downstream regions, the weathering of sedimentary rocks plays a greater role, and the anthropogenic effect suddenly becomes the most important factor influencing the chemistry of the river water at the lower reaches near Daegu. Substantial precipitation effects on the isotopes of oxygen, hydrogen, and nitrogen, and major ions were observed as well. Because this river is the largest tributary of the Nakdong River, its influence on the geochemistry of the latter is expected to be significant. It is also important to compare the geochemistry of the Nakdong River to that of the Han River because both rivers are two major rivers in Korea, and the lithologies of their drainage basins and land uses are very different. The catchment area of the Nakdong River is characterized by hilly forests, agricultural lands, and densely populated large cities including industrial complexes, while that of the Han River mainly consists of mountain areas. However, no geochemical data on the Nakdong River have been reported yet.

In this study, chemical composition and isotope data are obtained for the Nakdong River for the first time, and the effects of different factors such as weathering and anthropogenic activities on the chemical compositions and isotope variations of the river waters are discussed. Although isotope data for Sr and other isotopes, and chemical data have been usefully applied for the estimation of multiple processes in rivers, including anthropogenic input and chemical weathering (Xu et al., 2011; Zieliński et al., 2017;

Fig. 1 Geologic map and sampling locations around the Nakdong River



Négre et al., 2020), usually a single isotope has been used to study the geochemistry of river waters. We investigated various isotopes, such as hydrogen, oxygen, strontium, and carbon, as well as the chemical composition of the Nakdong River water, to contribute to understanding the weathering and land use factors controlling geochemistry and each isotope value in major rivers.

Materials and methods

Materials

The catchment area is characterized by hilly forests, agricultural lands, and industrial complexes from the headwater to Daegu. Daegu is a highly populated city with a population of approximately 2.47

million. Beyond Daegu, the catchment area is mainly composed of agricultural lands and small-scale factory areas. Figure 1 shows the simplified geological map and sampling locations of the Nakdong River basin. The Precambrian Sobagsan Gneiss Complex of Yongnam Massif that lies in the north-western part of the river mainly comprised high-grade paragenesis, including biotite gneiss and granitic gneiss, and subordinately of banded gneiss, migmatitic gneiss, mica schist, and orthogneiss (Park et al., 2006). The granitic rocks in this area are composed of the Daebo (Triassic to Jurassic) and Bulguksa (Cretaceous to Early Tertiary) granites. The former is located in the northern and eastern parts of the basin, and the latter is located in its south-eastern part. The Cretaceous non-marine sedimentary strata and intermediate-to-acidic volcanic rocks are the main sedimentary rocks distributed in this area (Chang, 1975).

Methods

Sampling

To investigate the precipitation effects and spatial variations of the chemical compositions and isotopes of both the Nakdong River and its tributary waters, water samples were collected three times during the autumn (November 2009), spring (May 2010), and summer (July 2010) seasons. The sampling period was determined by considering the precipitation rate because only July belonged to the rainy season in Korea. A total of 23 samples were collected; 13 samples were obtained along the main channel of the Nakdong River, and 10 samples—from its tributaries. The pH and electric conductivity (EC) of the water were measured during sampling using an Orion 290A pH meter and a 250A Trans Instruments EC meter, respectively. The obtained water samples were filtered through 0.45- μm cellulose nitrate membrane filters and stored in pre-cleaned 100-mL high-density polyethylene bottles with screw caps. Three different bottles were prepared for each sample to analyze the cations and anions as well as various isotopes of oxygen, deuterium, and strontium. The water samples for cation analysis were acidified below pH=2 using a 1-N HNO_3 solution to avoid precipitation and adsorption on the bottle walls. All samples were stored in an icebox, transported to a laboratory, and kept in a

refrigerator until analysis. Alkalinity was measured on the day of sampling following the Gran titration technique (Dyrssen and Sillen, 1967; Edmond, 1970). The accurate concentration of HCl ($\sim 0.05\text{ N}$) used for the titration was calibrated using a standard solution (1000 μN in alkalinity) that was prepared using NaHCO_3 (Kim et al., 2018). The content of dissolved inorganic carbon (DIC) was calculated from the pH and alkalinity data.

Water analysis

The presence of cations (Ca^{2+} , Na^+ , Mg^{2+} , and K^+) and Si in the water samples was determined by inductively coupled plasma atomic emission spectroscopy (Jobin Yvon Ultima 2) at the Seoul Centre of the Korean Basic Science Institute, and the presence of anions (SO_4^{2-} , Cl^- , NO_3^- , NO_2^- , and PO_4^{3-}) was analyzed by ion chromatography (Dionex ICS-5000) at the Kyungpook National University. Quantification limits for ICP analysis are generally 0.1 mg/L and those for IC analysis are approximately 0.01 mg/L. The precision and accuracy for ion analysis were verified by analyzing duplicate samples and by calculating charge balance errors. Most samples showed charge balance errors within $\pm 8\%$.

For carbon isotope analysis, river water samples were collected using evacuated glass septum vials, which were pre-filled with 85% phosphoric acid. CO_2 gas was extracted by a gas evolution technique and then cryogenically purified. To conduct the oxygen isotope analysis, 2 mL of the sample was equilibrated with CO_2 by shaking for 6 h at 25 °C. For the hydrogen isotope analysis, metallic zinc was used to produce hydrogen gas via a zinc reduction method. The oxygen, hydrogen, and carbon isotopic compositions of the water samples were determined using the VG Prism II stable isotope ratio mass spectrometer at the Korean Basic Science Institute. The analytical reproducibility was $\pm 0.1\text{‰}$ for $\delta^{18}\text{O}$, $\pm 1\text{‰}$ for δD , and $\pm 0.2\text{‰}$ for $\delta^{13}\text{C}_{\text{DIC}}$. For the Sr isotopic analysis, 60 mL of the sample was evaporated in ultraclean Teflon vessels and redissolved in distilled HCl solution. Strontium was separated from other ions in solution using cation exchange resin in a quartz column. Strontium isotopes were identified by the VG54-30 thermal ionization mass spectrometer at the Korean Basic Science Institute.

Statistical analysis

For bivariate statistical analysis, the Pearson correlation analysis was implemented to calculate the correlation coefficient (ρ) between the paired data (Table 2).

Results and discussion

Water geochemistry

The changes in the physico-chemical parameters and chemical compositions of the Nakdong River water with distance are listed in Table 1 (see also Figs. 2 and 3). The pH values of the river water along the flow path varied between of 7.19 and 9.13, indicating the absence of a visible trend. However, seasonal variations with average values of 8.07 in November, 8.24 in May, and 8.20 in July were observed, which could be attributed to the photosynthesis of aquatic plankton during summer (Lee et al., 2007). July belonged to the rainy season; as a result, this effect was slightly decreased by the dilution of the river water with rain.

The total dissolved cations and anions ($TZ^+ = Na^+ + K^+ + 2Mg^{2+} + 2Ca^{2+}$ and $TZ^- = Cl^- + 2SO_4^{2-} + NO_3^- + HCO_3^-$, respectively) in the river water were generally balanced, and their charge balances were normally maintained within $\pm 8\%$. The concentrations of most dissolved ions exhibit similar trends with the flow distance: first increasing slightly until a 300-km station influenced by both weathering and agricultural activities and then demonstrating more rapid increases with the inflow of high concentrations of dissolved ions from the Kumho River (especially for Na and SO_4 , which are considered pollutant ions; Figs. 2 and 3). The concentrations of Ca, Na, Mg, and K in the main stream were in the range of 10.7–34.2, 3.1–64.1, 2.4–9.5, and 1.8–11.2 mg/L, respectively. The Kumho River flows near the industrial complex in Daegu, the fourth largest city in Korea, and is significantly influenced by the sewage treatment plant of a dyeing industrial complex (Kim & Kim, 2013). From stations 13–15, the mean concentration of Na increased abruptly from 17.3 to 41.4 mg/L, affected by the river water of the Kumho River (station 14, 99.8 mg/L). Before sampling station 15, the mean cation concentrations in the main stream were ranked in the order of $Ca (21.5 \text{ mg/L}) > Na$

$(10.2 \text{ mg/L}) > Mg (5.8 \text{ mg/L}) > K (3.1 \text{ mg/L})$, but afterwards, the order changed to $Na (29.1 \text{ mg/L}) > Ca (22.6 \text{ mg/L}) > Mg (6.8 \text{ mg/L}) > K (5.6 \text{ mg/L})$, which was especially more pronounced in November). This order of cation concentrations is almost identical to that at the lower reaches of the Kumho River before the latter meets the Nakdong River at Daegu. However, the cation concentrations in the Kumho River were higher than those in the Nakdong River, indicating that after this station, the geochemistry of the river water was greatly affected by that of the Kumho River and a dyeing industrial complex, although its ion concentrations were partially lowered by dilution. However, after this station, the river water was still influenced by two sewage treatment plants and an auto parts industrial complex in Daegu. Among various cations, Na exhibited the highest increase after this station (especially in November), strongly suggesting its anthropogenic origin. In May and July, the corresponding Ca concentrations were close to those of Na after station 15.

The anions also exhibited a similar trend. The concentrations of HCO_3^- , SO_4^{2-} , Cl, and NO_3^- in the main stream were in the range of 30.0–88.6, 11.9–104.5, 4.5–70.1, and 0.6–17.7 mg/L, respectively. Before station 15, their mean concentrations ranked in the order of $HCO_3^- (57.3 \text{ mg/L}) > SO_4^{2-} (24.7 \text{ mg/L}) > Cl (15.6 \text{ mg/L}) > NO_3^- (7.9 \text{ mg/L})$, but from station 15, the order did not change (the mean concentrations of HCO_3^- , SO_4^{2-} , Cl, and NO_3^- were 62.8, 44.6, 34.9, and 10.8 mg/L, respectively). However, in November and May, the concentration of SO_4^{2-} abruptly increased at station 15 and became close to that of HCO_3^- . The mean concentration of SO_4^{2-} at station 13 increased from 26.7 to 61.7 mg/L, mainly influenced by the river water of the Kumho River (144.8 mg/L) and a dyeing industrial complex. Although the ion concentrations in the river were greater than the average values obtained for various rivers around the world (Holland, 1978), the content of HCO_3^- ions, which was a weathering product (along with Ca species), was within the range obtained for the world rivers (Gaillardet et al., 1999) and slightly higher than that of the North Han River, but close to the magnitude determined for the South Han River (Lee et al., 2007).

The reported concentrations of SO_4^{2-} ions in the Kumho River were higher than those of the anions present in that river, and the inflow of the Kumho River water was supposedly the main reason for the

Table 1 Physical and chemical properties and isotope compositions of the water samples in Nakdong River (O: main stream, X: tributary)

Station	Distance (km)	pH	EC (µ/cm)	Alkalinity (meq/L)	K (mg/L)	Ca (mg/L)	Mg (mg/L)	Na (mg/L)	Si (mg/L)	HCO ₃ (mg/L)	Cl (mg/L)	NO ₃ (mg/L)	SO ₄ (mg/L)	d ¹⁸ O (‰)	d ² H (‰)	d ¹³ C _{DIC}	⁸⁷ Sr/ ⁸⁶ Sr	
November																		
P1	O 23.50	8.20	302	0.90	3.4	31.3	8.7	12.7	10.3	54.6	19.9	8.1	88.3	-8.66	-61.6	-7.1	0.72627	
P2	X 43.48	8.11	257	1.23	2.9	21.7	7.7	9.0	13.3	74.7	9.8	6.3	20.9	-8.10	-61.5	-12.6	0.71119	
P3	O 65.33	8.23	407	0.64	2.4	15.0	4.5	6.2	2.9	39.2	4.5	0.6	23.1	-8.75	-64.6	-9.0	0.72195	
P4	O 85.78	8.25	392	0.80	3.4	17.9	5.7	9.0	4.6	49.1	9.0	7.2	23.5	-8.63	-63.4	-10.1	0.71897	
P5	X 105.75	8.18	418	1.32	4.4	20.6	6.3	17.5	23.3	80.7	14.4	8.8	21.2	-7.74	-56.2	-11.3	0.71985	
P6	X 126.90	8.46	540	0.53	3.2	16.0	4.9	9.8	21.5	32.3	11.0	8.8	23.7	-8.15	-60.1	-10.3	0.71913	
P7	X 146.88	8.56	361	1.70	4.3	29.4	9.9	17.0	13.2	103	24.0	4.3	40.7	-7.62	-56.2	-10.6	0.71646	
P8	O 167.79	7.78	258	1.00	3.2	19.1	6.2	11.5	18.7	60.8	12.0	11.0	25.83	-8.08	-60.1	-11.5	0.71786	
P9	X 188.00	8.49	265	1.37	5.7	27.7	10.8	14.5	7.1	83.6	32.1	2.6	44.2	-6.33	-50.6	-11.7	0.71289	
P10	O 209.15	7.84	215	1.14	4.8	21.9	6.7	12.3	12.9	69.6	32.3	7.2	25.0	-7.98	-57.9	-11.0	0.71766	
P11	X 229.13	7.72	217	1.57	8.8	25.5	7.3	29.5	26.6	95.7	44.7	16.1	25.8	-7.78	-57.5	-11.9	0.71243	
P12	O 250.51	7.74	268	1.10	4.8	21.9	6.4	15.1	13.7	67.6	13.6	6.2	20.1	-7.84	-56.2	-11.4	0.71691	
P13	O 270.25	7.87	368	1.11	5.7	32.5	7.2	22.0	11.7	67.9	28.5	9.1	38.3	-7.90	-58.7	-11.3	0.71618	
P14	X 291.40	7.79	1170	1.95	25.8	82.3	32.5	158	18.8	119	138	28.1	276.7	-7.40	-54.8	-12.0	0.71041	
P15	O 312.32	7.96	605	1.45	11.2	28.5	9.5	64.1	7.6	88.6	70.1	17.7	104.5	-7.70	-57.7	-11.1	0.71297	
P16	O 333.00	8.57	578	1.40	10.9	28.1	9.2	52.0	18.8	85.4	60.0	14.4	89.8	-7.72	-58.5	-11.1	0.71321	
P17	X 353.68	7.93	170	0.58	2.5	9.9	4.0	7.8	13.8	35.5	9.1	4.5	7.2	-8.23	-61.5	-9.9	0.71189	
P18	O 373.65	8.13	505	1.27	7.8	23.8	8.2	48.6	2.9	77.3	56.2	12.0	84.2	-7.79	-58.2	-11.3	0.71263	
P19	X 394.80	8.70	434	1.21	5.5	19.7	13.5	22.3	1.7	73.7	29.3	6.0	69.3	-6.67	-49.7	-8.8	0.71271	
P20	O 415.95	7.19	799	1.34	7.6	25.2	9.5	48.2	6.5	81.6	55.4	12.0	85.8	-7.49	-57.0	-11.6	0.71265	
P21	X 435.93	7.87	294	0.88	7.8	19.7	6.8	20.8	12.8	53.8	23.8	9.4	37.8	-6.75	-50.9	-9.2	0.70691	
P22	O 455.90	7.88	466	1.37	7.7	25.1	9.1	43.4	1.3	83.5	48.7	9.5	77.4	-7.39	-56.2	-11.4	0.71248	
P23	O 477.05	8.23	395	1.21	7.0	22.7	8.1	25.6	0.8	73.9	38.0	7.8	46.5	-7.25	-54.4	-10.9	0.71239	
May																		
P1	O 23.50	8.49	112	0.51	1.8	10.7	2.4	3.1	9.9	31.1	6.6	6.8	11.9	-9.13	-63.2	-5.6	0.71721	
P2	X 43.48	7.87	148	0.60	2.7	13.6	3.5	4.3	9.2	36.0	11.9	9.9	12.5	-7.88	-57.7	-10.0	0.71775	
P3	O 65.33	7.97	150	0.89	2.3	22.6	5.4	8.2	13.7	54.3	11.0	8.2	24.3	-8.45	-61.8	-8.0	0.71261	
P4	O 85.78	7.93	200	0.95	2.3	22.0	6.2	8.3	5.6	57.9	12.7	8.7	20.1	-8.30	-61.4	-8.9	0.71796	
P5	X 105.75	8.20	117	0.86	1.9	13.4	3.1	5.4	10.4	52.5	8.8	8.4	7.6	-8.40	-58.9	-9.4	0.71346	
P6	X 126.90	8.75	165	0.73	2.5	14.7	4.0	9.0	15.6	44.7	12.3	10.2	12.7	-8.23	-58.4	-8.7	0.71857	

Table 1 (continued)

Station	Distance (km)	pH	EC (µ/cm)	Alkalinity (meq/L)	K (mg/L)	Ca (mg/L)	Mg (mg/L)	Na (mg/L)	Si (mg/L)	HCO ₃ (mg/L)	Cl (mg/L)	NO ₃ (mg/L)	SO ₄ (mg/L)	d ¹⁸ O (‰)	d ² H (‰)	d ¹³ C _{DIC}	⁸⁷ Sr/ ⁸⁶ Sr	
P7	X 146.88	7.84	155	0.48	1.9	15.2	4.4	6.1	13.3	29.3	12.1	8.7	12.4	-8.29	-56.0	-11.1	0.71736	
P8	O 167.79	7.91	173	0.73	2.3	18.0	4.8	8.2	6.3	44.5	14.4	11.6	15.8	-8.19	-57.6	-8.9	0.72038	
P9	X 188.00	8.29	310	1.34	4.2	34.3	10.0	14.1	5.6	81.8	24.5	8.3	27.9	-6.63	-50.1	-10.1	0.72218	
P10	O 209.15	8.02	186	1.06	2.4	19.6	5.5	8.7	5.3	64.9	13.7	9.3	16.5	-8.07	-58.0	-8.7	0.71882	
P11	X 229.13	8.07	256	1.23	4.0	17.8	4.9	22.1	8.1	75.3	29.2	14.8	13.9	-8.18	-60.0	-10.5	0.72208	
P12	O 250.51	8.10	181	1.02	2.5	16.5	5.3	8.8	12.2	62.3	12.8	9.4	15.2	-8.11	-57.3	-8.6	0.71207	
P13	O 270.25	7.76	208	0.85	3.1	17.9	5.4	11.7	19.8	51.7	17.5	10.6	19.1	-8.07	-56.7	-8.8	0.72658	
P14	X 291.40	7.94	661	2.99	9.5	41.2	11.6	82.7	6.2	182.7	71.6	14.1	91.4	-7.14	-50.5	-11.3	0.70997	
P15	O 312.32	9.00	341	0.50	3.6	23.7	6.4	25.1	10.6	30.9	33.7	11.7	38.4	-7.68	-54.0	-9.0	0.71378	
P16	O 333.00	8.39	308	0.62	3.2	21.9	6.4	20.8	9.1	37.9	27.6	12.1	31.9	-7.65	-55.7	-8.4	0.71459	
P17	X 353.68	7.86	140	0.42	2.9	8.8	2.0	5.3	3.4	25.8	13.5	8.0	7.4	-7.76	-56.2	-9.3	0.71169	
P18	O 373.65	8.10	241	0.78	3.5	19.6	5.6	18.5	1.1	47.3	24.2	10.3	21.9	-7.72	-55.5	-8.6	0.71315	
P19	X 394.80	7.69	133	0.19	2.0	7.2	2.5	4.8	8.9	11.5	13.0	8.8	11.8	-7.15	-48.6	-8.7	0.71278	
P20	O 415.95	8.50	270	1.02	4.3	22.0	6.6	21.7	9.5	62.3	26.7	9.7	26.6	-7.53	-53.4	-8.2	0.71304	
P21	X 435.93	8.78	192	0.59	3.2	11.1	3.3	8.5	13.6	36.0	15.7	9.3	14.8	-7.03	-48.4	-12.0	0.70711	
P22	O 455.90	8.79	236	0.55	3.5	13.8	3.9	12.1	1.8	33.8	24.5	8.7	24.0	-7.37	-51.1	-8.5	0.71323	
P23	O 477.05	9.31	253	0.56	3.8	19.0	5.3	18.3	2.2	34.0	25.8	8.7	25.3	-7.33	-50.6	-8.4	0.71250	
July																		
P1	O 23.50	8.29	245	1.22	2.2	27.7	6.2	12.8	12.5	74.5	14.0	5.4	35.8	-8.73	-65.8	-10.02	0.72660	
P2	X 43.48	7.88	204	1.25	2.2	23.6	6.8	6.7	14.1	76.3	12.3	8.4	13.1	-7.91	-60.3	-12.81	0.71220	
P3	O 65.33	8.14	199	0.76	2.0	16.3	4.4	4.2	19.4	46.4	9.76	6.0	15.2	-8.23	-61.2	-11.15	0.71739	
P4	O 85.78	8.53	225	0.63	4.3	19.7	4.2	10.7	9.5	38.3	15.3	7.9	22.4	-8.24	-61.4	-10.46	0.71789	
P5	X 105.75	8.84	265	1.21	3.4	23.7	5.0	12.5	27.3	74.1	17.4	7.3	16.6	-7.68	-59.5	-12.58	0.71988	
P6	X 126.90	8.13	296	1.08	2.4	30.0	7.8	9.2	36.8	65.6	15.8	29.2	19.7	-7.69	-57.8	-12.53	0.71795	
P7	X 146.88	8.84	255	1.40	3.0	28.1	7.0	8.1	22.9	85.9	19.1	5.7	16.1	-8.07	-57.7	-13.39	0.71644	
P8	O 167.79	8.34	244	1.07	2.8	25.1	6.2	7.8	20.9	65.1	19.7	9.1	19.3	-8.06	-58.7	-11.71	0.71716	
P9	X 188.00	8.28	304	1.25	4.0	35.0	9.0	7.6	20.2	76.5	20.4	8.4	24.0	-7.74	-58.2	-12.66	0.71295	
P10	O 209.15	8.62	249	1.01	3.5	25.1	6.6	7.3	6.3	61.7	16.5	6.9	18.0	-7.92	-59.5	-11.26	0.71577	
P11	X 229.13	8.10	284	1.27	5.2	21.5	5.7	12.1	36.4	77.7	25.1	12.2	14.8	-8.72	-61.6	-13.46	0.71244	
P12	O 250.51	8.55	259	1.13	3.7	24.3	6.6	7.5	41.7	68.9	19.1	8.4	17.7	-7.98	-59.1	-11.60	0.71462	
P13	O 270.25	8.62	297	1.19	4.7	27.2	6.7	18.1	34.0	72.8	24.5	7.7	22.8	-7.99	-56.6	-11.53	0.71444	

Table 1 (continued)

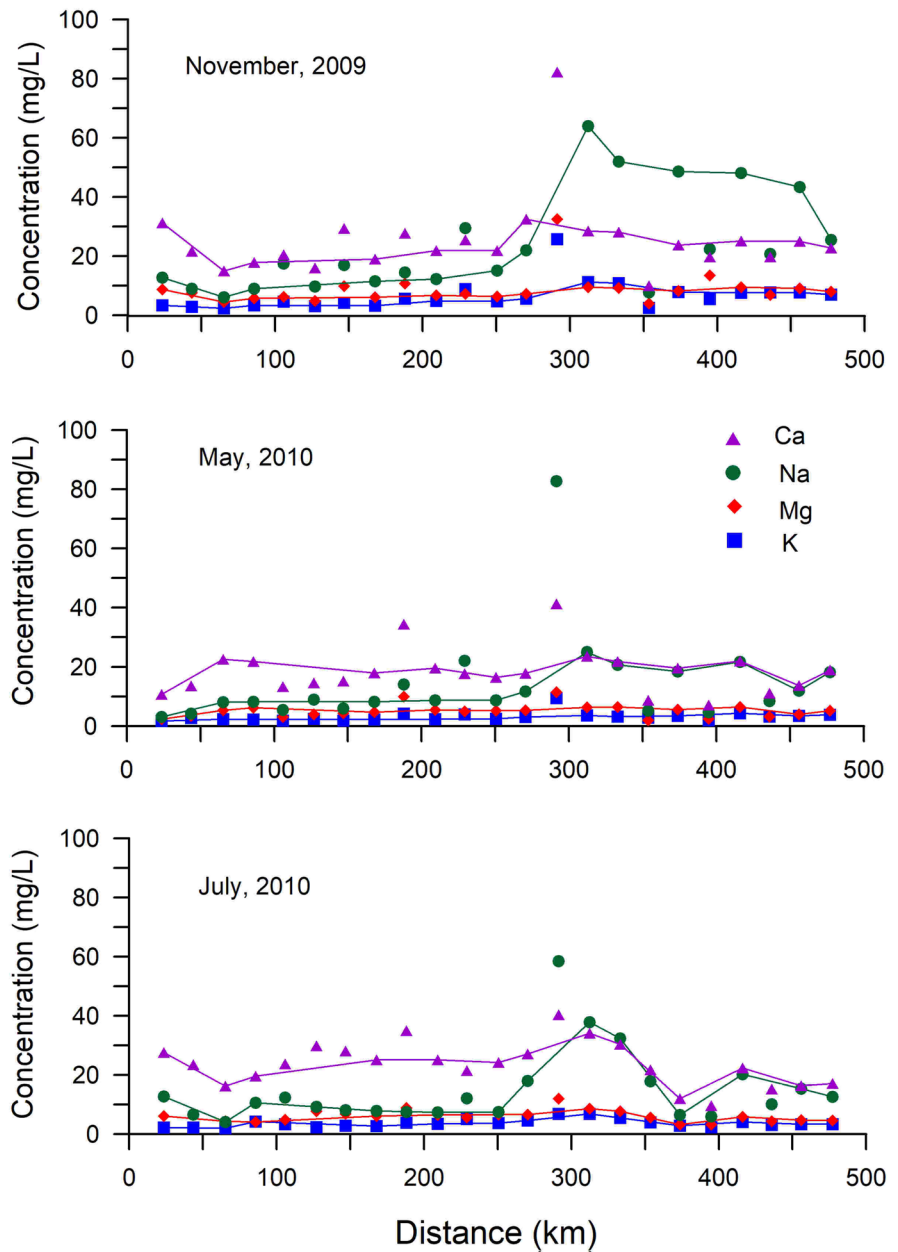
Station	Distance (km)	pH	EC (µ/cm)	Alkalinity (meq/L)	K (mg/L)	Ca (mg/L)	Mg (mg/L)	Na (mg/L)	Si (mg/L)	HCO ₃ (mg/L)	Cl (mg/L)	NO ₃ (mg/L)	SO ₄ (mg/L)	d ¹⁸ O (‰)	d ² HD (‰)	d ¹³ C _{DIC}	⁸⁷ Sr/ ⁸⁶ Sr
P14	X 291.40	7.20	525	1.74	6.9	40.5	12.0	58.6	23.0	106	51.1	19.5	66.4	-8.15	-58.6	-13.26	0.71009
P15	O 312.32	7.86	481	1.51	6.9	34.2	8.6	38.0	10.0	92.5	36.8	14.6	42.1	-8.19	-59.1	-12.55	0.71158
P16	O 333.00	7.90	409	1.36	5.5	30.4	7.8	32.4	16.4	83.1	35.6	13.7	37.2	-8.20	-58.1	-12.94	0.71207
P17	X 353.68	7.79	302	1.36	4.0	21.8	5.7	17.8	13.6	83.0	21.1	9.3	21.0	-8.40	-61.7	-13.13	0.71170
P18	O 373.65	7.87	171	0.66	2.9	12.1	3.3	6.5	17.0	40.1	9.4	6.4	7.7	-8.48	-62.2	-13.78	0.71133
P19	X 394.80	7.89	236	0.50	2.3	9.7	3.3	6.0	41.3	30.5	9.1	5.8	10.6	-8.51	-60.7	-11.52	0.71307
P20	O 415.95	7.75	321	1.12	4.1	22.5	5.9	20.3	41.7	68.5	21.4	9.8	23.8	-8.36	-60.6	-13.14	0.71184
P21	X 435.93	8.02	220	0.86	3.1	15.2	4.5	10.1	26.0	52.7	15.2	11.9	16.0	-7.82	-57.7	-11.95	0.70731
P22	O 455.90	8.03	245	0.82	3.5	16.4	4.8	15.5	22.4	50.3	16.4	7.9	17.7	-8.32	-59.9	-12.34	0.71168
P23	O 477.05	9.13	330	0.96	3.4	17.1	4.7	12.6	21.8	58.5	17.9	7.9	17.4	-8.28	-61.1	-11.78	0.71188

observed increase in the SO₄ concentration after the station. These ions can have many different anthropogenic sources (Lang et al., 2011; Li et al., 2011; Ryu et al., 2007; Zhang et al., 1995), and no evaporite deposits were detected in the sedimentary basin around this river (Chang, 1975). Therefore, similar to Na ions, SO₄ ions originated from anthropogenic sources. Ryu et al. (2007) reported the SO₄ concentrations and sulfur isotope values of the river waters from the two tributaries of the Han River and attributed the major source of SO₄ ions in the North Han River to the atmospheric input based on the concentration range (3.8–8.6 mg/L) and δ³⁴S values. They also concluded that the SO₄ concentrations in the river waters flowing from the South Han River (3.8–30.7 mg/L) were higher than that from the atmospheric input and attributed the origin of SO₄ ions to the oxidation of sulfides in an abandoned mine and coal-bearing sedimentary rocks based on the δ³⁴S values. Although we did not measure δ³⁴S values, the SO₄ concentrations in the Kumho River were generally higher than those in the North Han River. Considering the much higher SO₄ concentrations in the river water after the inflow of the Kumho River, which is severely influenced by industrial activities, the presence of SO₄ ions before station 15 can be mainly attributed to the oxidation of pyrite in the sedimentary rocks and fertilizers in the upstream region influenced by agricultural activities (Brenot et al., 2007; Lee et al., 2007). After the inflow of the Kumho River, other anthropogenic products generated by the sewage treatment plant and industrial complex became more important, especially in November (Li et al., 2011). As with cations, the anions after this station are also influenced by two additional sewage treatment plants and auto parts industrial complex.

The mean values of NO₃ concentrations, which also had anthropogenic sources, were equal to 9.44, 9.92, and 9.96 mg/L in November, May, and July, respectively, and did not significantly change after the inflow of the Kumho River water, suggesting a variety of agricultural origins. They are close to the magnitudes obtained for the South Han River, which flows through the agricultural areas, but higher than the values measured for the North Han River flowing through the mountains.

The relative contents of the major ions are plotted in the anion and cation ternary diagram and Piper diagram depicted in Figs. 4 and 5. The water data were

Fig. 2 Comparison of the major cations in the water samples collected at different sampling stations along the Nakdong River. The lines show the data from the main stream

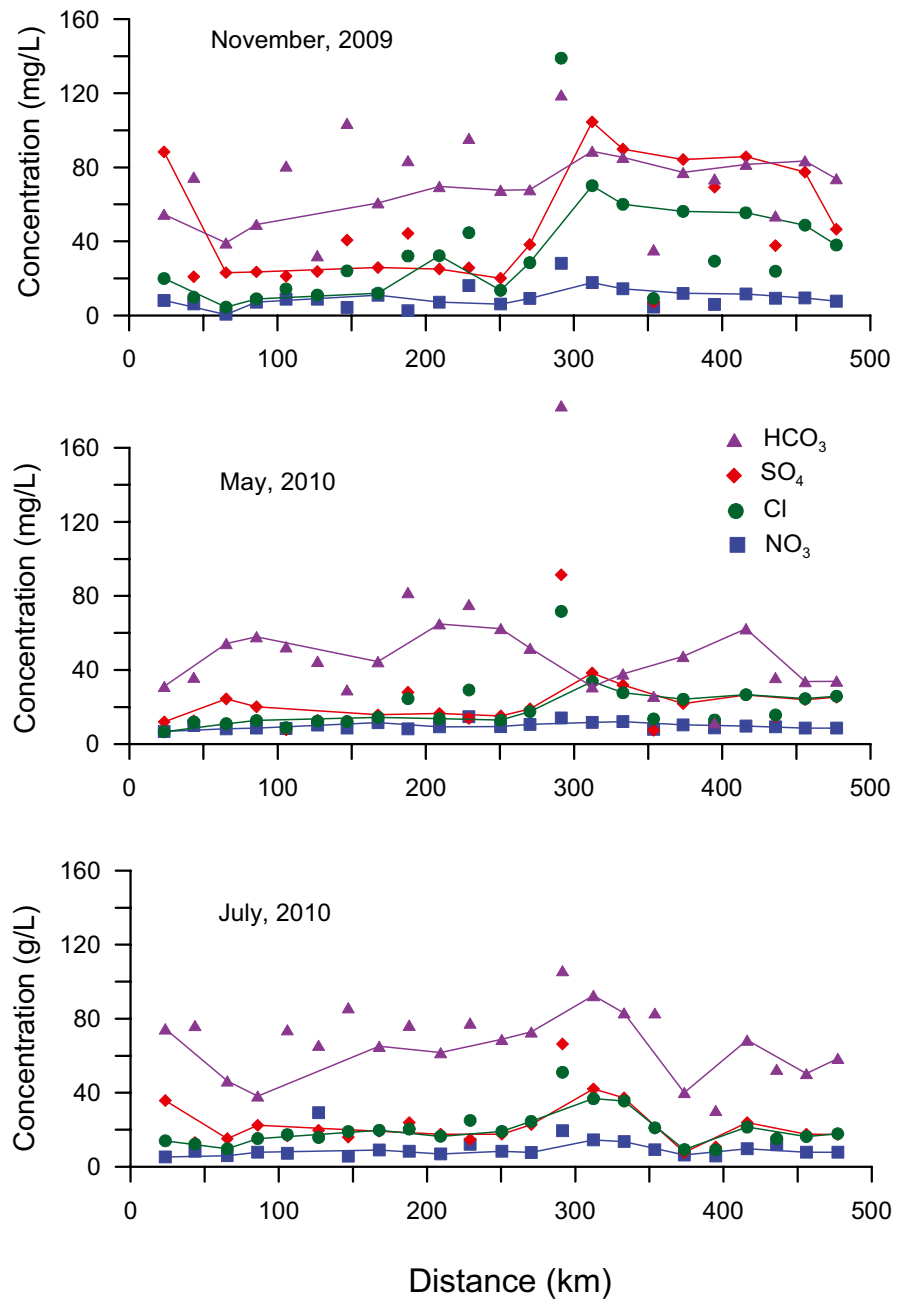


plotted slightly different regions in the two diagrams, indicating that the water chemistry is influenced to some extent by the precipitation rate. They show that in July, the relative concentrations of Cl and SO₄ and Na and K species, which were more closely related to the anthropogenic effects, clearly decreased due to rainwater. However, no noticeable differences between the relative ion concentrations in November and May were observed.

Oxygen and hydrogen isotopes

Previous studies showed that δ¹⁸O and δD could be good indicators of the origin or mixing of waters in rivers (Kendall & Coplen, 2001; Lambs, 2000; Winston & Criss, 2003; Barth & Veizer, 2004; Li et al., 2016). The two isotope compositions of the Nakdong River plotted in Fig. 6 are close to the global meteoric water line, but slightly below the local meteoric water line. The

Fig. 3 Comparison of the major anions in the water samples collected at different sampling stations along the Nakdong River



corresponding $\delta^{18}\text{O}$ and δD values range from -9.13 to -6.33 and -65.8 to -48.4‰ with the means of -7.92 and -57.7‰ , respectively (Table 1). However, the isotopic values had different ranges and mean values in different seasons. The river waters were lightest and least scattered during July than during other seasons. In general, the annual temperature cycle is the main factor affecting the isotopic variations of precipitation in

different seasons with the highest value observed during summer (Clark & Fritz, 1997; Fricke & O'Neil, 1999; Hoefs, 2004). In contrast, the precipitation in Korea generally exhibits the lowest isotopic concentrations during summer and the highest ones during winter, which is mainly due to tropical cyclones and downpours (Lee & Chang, 1994; Lee et al., 2003), which was also observed for the Nakdong River with lower

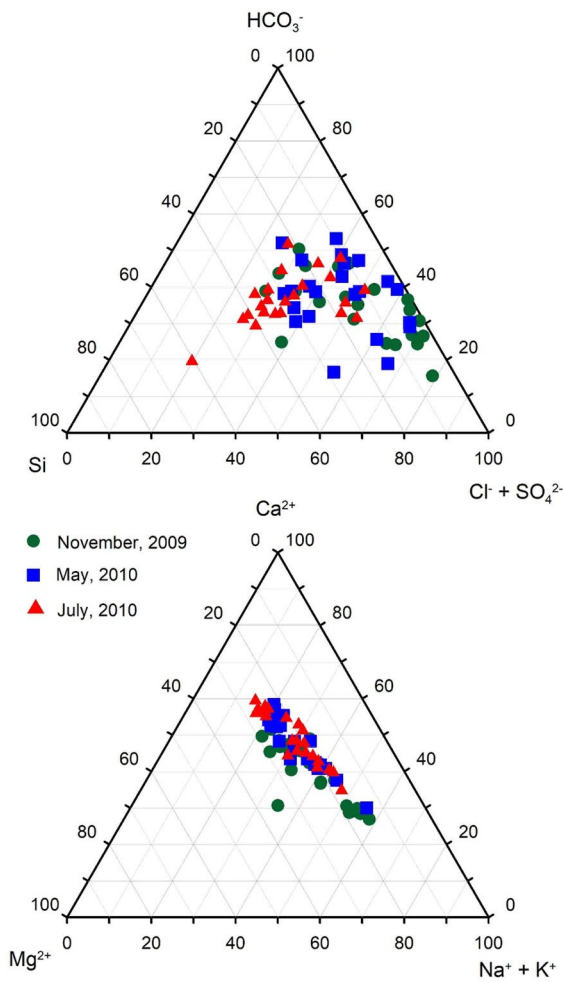


Fig. 4 Ternary diagrams showing the anion and Si (upper panel) and cation (lower panel) compositions

isotopic concentrations in July, indicating that different sources of precipitation and downpours were the probable reasons for the lower values. These results are different from the isotopic data obtained for the Kumho River (Kim & Kim, 2013) and for the North and South Han Rivers (Ryu et al., 2007). The highest $\delta^{18}\text{O}$ and δD values measured for the Kumho River during summer were attributed to the severe water evaporation from a dam at high temperatures. The large $\delta^{18}\text{O}$ and δD magnitudes obtained for the North and South Han River waters also indicate a high evaporation level. The opposite trend observed for the $\delta^{18}\text{O}$ and δD values between the Nakdong River and Kumho River indicate that the ions dissolved in the Nakdong River were greatly

influenced by the Kumho River, but the $\delta^{18}\text{O}$ and δD values of the Nakdong River water were more strongly affected by the precipitation, although the evaporation effect was observed in November.

The $\delta^{18}\text{O}$ and δD values increased in the downstream (Fig. 7), showing high isotopic concentrations in the precipitation due to the preferential condensation of the isotopically heavier water vapor and rain at low altitudes (Clark & Fritz, 1997). This can also be due to the evaporative enrichment during downstream transport or evaporative enrichment of soil water in downstream areas. The relationship between the $\delta^{18}\text{O}$ and δD values and altitude showed that during November and May, the isotope values decreased with increasing altitude (Fig. 7). However, during July, this trend is unclear, which can be interpreted as a result of dilution of those effects by high precipitation rate.

Stable isotope analyses can provide important information on the origins and evaporative history of urban water supplies impacted by human activities. Li et al. (2019) reported that $\delta^{18}\text{O}$ and δD values of river water in urban areas are higher than those in non-urban areas depending on the degree of river development and utilization. In our study area, particularly in May, the increase of those two isotopic values was observed after 300 km, at which point the river water was influenced by the urban area (Daegu). This increase can be explained by the anthropogenic effects, because the river water may be least affected by precipitation during in May. During November and July, this effect was not clear.

Strontium isotope

Strontium isotope compositions in water are influenced by the differential weathering rates of different minerals in the rock (Bataille & Bowen, 2012; Bataille et al., 2014). For example, more reactive minerals or rocks such as carbonate, evaporite, and basalt can have more influence on the $^{87}\text{Sr}/^{86}\text{Sr}$ ratio in water. Therefore, the $^{87}\text{Sr}/^{86}\text{Sr}$ ratio in water can differ from that of the bedrock. The different abundances of ^{87}Sr and resultant $^{87}\text{Sr}/^{86}\text{Sr}$ ratios are caused by the formation of the isotope ^{87}Sr through the radioactive decay of ^{87}Rb and can vary due to the chemical fractionation between Rb and Sr as well as to the elapsed time in the closed system. Therefore, the $^{87}\text{Sr}/^{86}\text{Sr}$ ratio can be used as a parameter that helps to identify

Fig. 5 Piper diagram of water chemistry for the Nakdong River

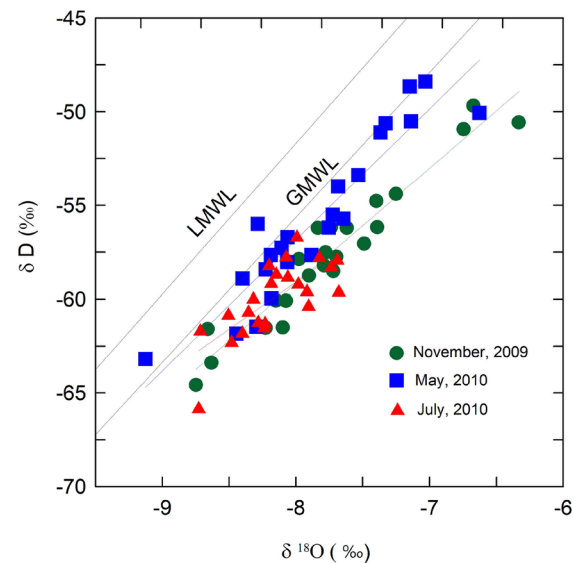
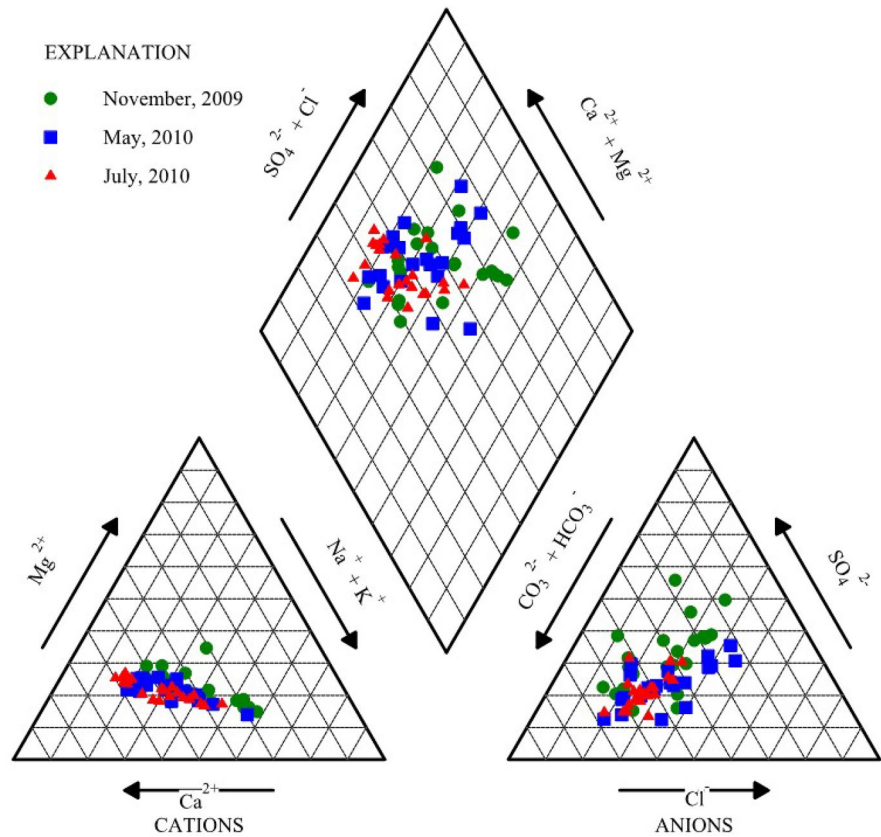


Fig. 6 δD plotted as a function of $\delta^{18}O$ for the water samples collected during three different seasons

the sources of dissolved ions in river waters (Andrew et al., 2016; Brennan et al., 2014).

The $^{87}Sr/^{86}Sr$ ratio of the Nakdong River water generally decreased downstream in the range of 0.70691~0.72660 with mean values of 0.71507, 0.71560, and 0.71429 obtained in November, May, and July, respectively (Fig. 8). These magnitudes are very close to each other, and no noticeable seasonal variations were observed. The variations in the $^{87}Sr/^{86}Sr$ ratio resulted from the weathering of different rock types. The geology of the study area is very complex, and in the upstream region, it was influenced by both the granitic and gneissic rocks and partially by the sedimentary rocks. Flowing downstream, the river waters were more strongly affected by the sedimentary rocks. Lee et al. (2007) measured Sr isotope values in the two large tributaries of the Han River and found that the North Han River was influenced by the weathering of granite with a higher $^{87}Sr/^{86}Sr$ ratio and the South Han River—by the carbonate and sedimentary rocks with lower $^{87}Sr/^{86}Sr$ ratios. Most granitic metamorphic rocks have initial $^{87}Sr/^{86}Sr$ ratios in

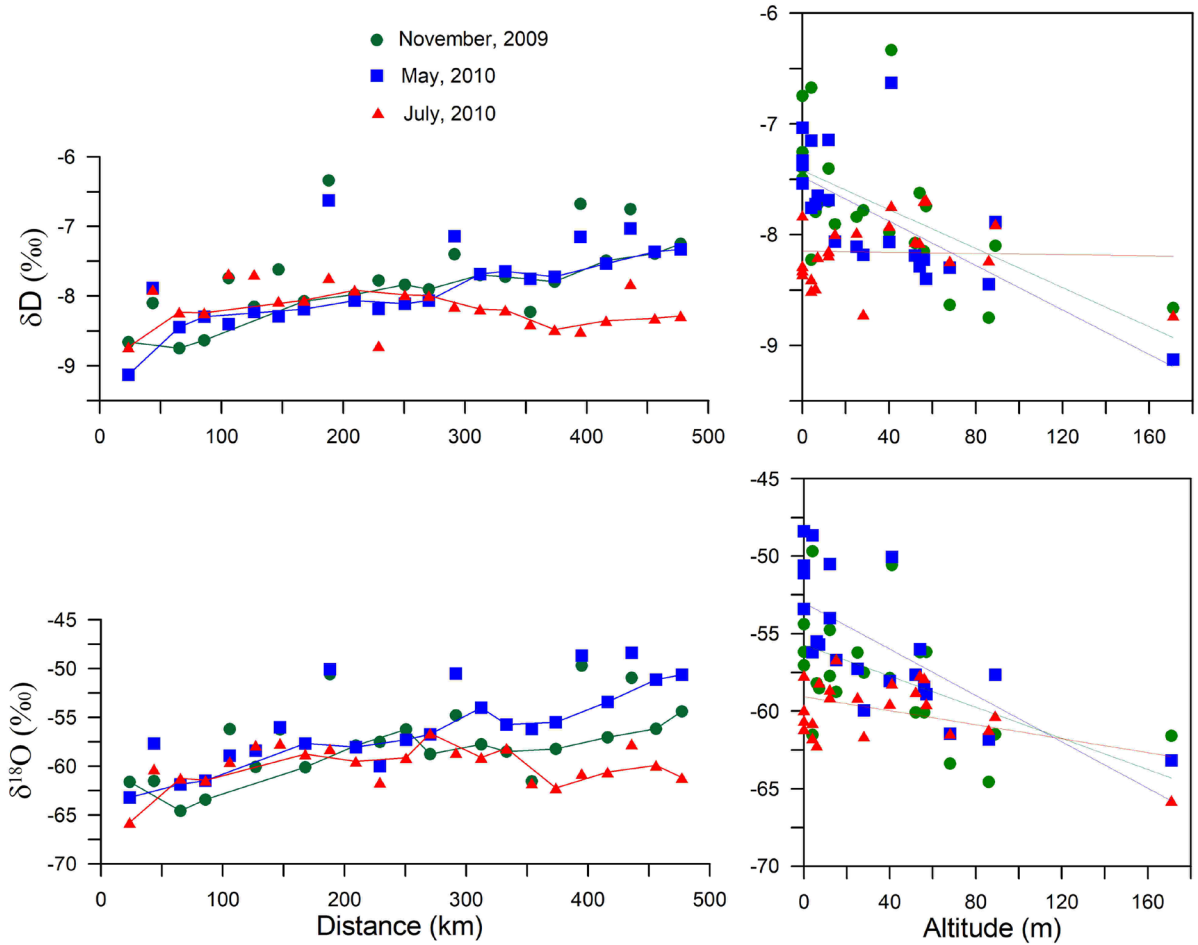
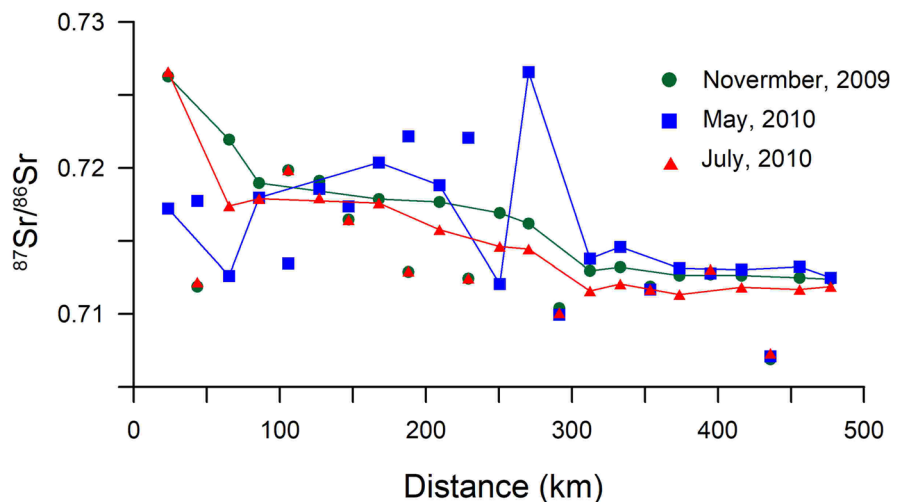


Fig. 7 Changes in the $\delta^{18}O$ and δD values of the water samples as functions of the distance from the first sampling station and the variations of $\delta^{18}O$ and δD values with altitude

Fig. 8 Changes in the $^{87}Sr/^{86}Sr$ ratios of the samples collected during three different seasons as functions of the distance from the first sampling station



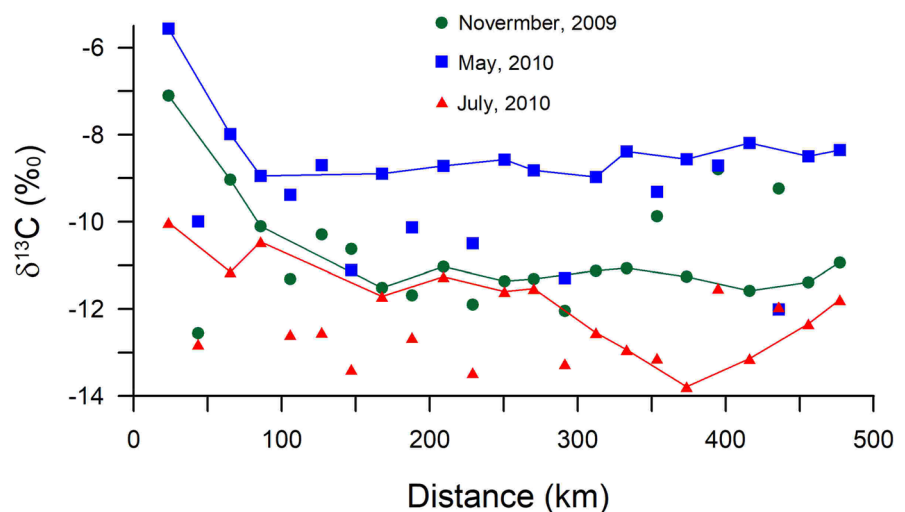
the range of 0.709–0.725, and limestones exhibit the ratio equal to that of seawater (0.706–0.709) (Faure, 1977; Bierman et al., 1998). The sedimentary rocks comprising the Nakdong River basin mostly consist of shale, sandstone, and conglomerate, which contain calcite components. These sedimentary rocks were deposited in a lacustrine environment, whose Sr isotope ratio might be different from those of the marine environments. However, considering the decrease in the $^{87}\text{Sr}/^{86}\text{Sr}$ ratios in the downstream of the Nakdong River, it is clear that these compositions in the sedimentary rocks are lower than those in the granitic and gneissic rocks, indicating that the weathering of rocks in river basins plays an important role in controlling their geochemical compositions; however, the contributions from various rock types are almost the same during different seasons. In May, before 300 km (P13), abrupt increase of $^{87}\text{Sr}/^{86}\text{Sr}$ ratio was observed. Considering there were no appreciable lithological changes, other anthropogenic factors maybe have caused this increase (Zieliński et al., 2021). That area is heavily cultivated, and the $^{87}\text{Sr}/^{86}\text{Sr}$ ratio of fertilizer was previously reported to be as high as 0.740 (Borg & Banner, 1996; Vitòria et al., 2004), suggesting that agricultural activity may increase $^{87}\text{Sr}/^{86}\text{Sr}$ at this location.

Carbon isotope

Many different factors including biogenic CO_2 , atmospheric CO_2 , and DIC resulting from carbonate weathering contribute to the $\delta^{13}\text{C}_{\text{DIC}}$ values of the river

water (Wachniew, 2006). The $\delta^{13}\text{C}_{\text{DIC}}$ values of the Nakdong River varied with the distance and season (Fig. 9). In the upstream regions, they were relatively high, especially during November ($-9.0 \sim -7.1\text{‰}$) and May ($-8.0 \sim -5.6\text{‰}$), but decreased abruptly and became relatively constant except for the month of July. The $\delta^{13}\text{C}_{\text{DIC}}$ values of the tributaries were lower than those of the mainstream in May and July, but not in November (they also varied during different seasons). The mean $\delta^{13}\text{C}_{\text{DIC}}$ values obtained in November, May, and July were -10.7 , -9.1 , and -12.24‰ , respectively. Their variations strongly indicate that the sources of DIC in the river water were different in the upstream regions and other areas. The high values of $\delta^{13}\text{C}_{\text{DIC}}$ suggest that ^{13}C -enriched carbonate-derived DIC, which is also equivalent to the weathering of the rocks, is the main source of DIC. However, the decrease in $\delta^{13}\text{C}_{\text{DIC}}$ with distance indicates the dominant input from the ^{13}C -depleted soil-derived DIC, which results from the CO_2 species derived from the root respiration and microbial decomposition of soil organic matter. Because weathering is the dominant process supplying ions and DIC into the river water in the upstream regions, their $\delta^{13}\text{C}_{\text{DIC}}$ values were relatively high. However, in the downstream regions, a larger amount of DIC originated from soils, which lowered the corresponding $\delta^{13}\text{C}_{\text{DIC}}$ values. Considering that most area is used for agricultural activities in the downstream regions, the main source of DIC in this area is anthropogenic activity (Barth et al., 2003). The other factors that can increase the $\delta^{13}\text{C}_{\text{DIC}}$ magnitude include the photosynthetic

Fig. 9 Variations of the $\delta^{13}\text{C}_{\text{DIC}}$ values of the water samples collected during three different seasons as functions of the distance from the first sampling station



assimilation of CO₂, which increases the ¹³C content in the DIC remained in water and CO₂ exchange with atmosphere. However, these processes do not appear to be dominant because of the constantly decreasing δ¹³C_{DIC} values with the flow distance, and the latter was reported to be a slow process even in the largest rivers (Ryu et al., 2007; Wachniew, 2006).

The variations of δ¹³C_{DIC} values in different seasons may result from the different oxidation rates of soil organic matter. In July, the highest oxidation rate and lowest δ¹³C_{DIC} value were observed due to the high temperature and high precipitation level. The high precipitation rate also reduces mineral–water reaction, lowering the contribution of weathering to δ¹³C_{DIC} value (Li et al., 2008). In November, the DIC produced during the summer still had an effect on the river water. However, in May, the oxidation of soil organic matter was limited through the winter; as a result, the highest δ¹³C_{DIC} values were obtained.

The δ¹³C_{DIC} values are plotted as functions of alkalinity (the HCO₃⁻ concentration) in Fig. 10. In general, negative correlations between these parameters were obtained. If the oxidation of organic matter is the main source of DIC in the river water, the corresponding δ¹³C_{DIC} values exhibit a negative correlation due to the increased alkalinity resulting from the increase in the ¹²C-enriched soil-derived DIC. If the sedimentary carbonates are a major source of

the riverine DIC, the obtained δ¹³C_{DIC} values show a positive correlation. In Fig. 9, only a small portion of the upstream regions exhibits relatively high δ¹³C_{DIC} values suggesting that weathering was the main DIC source only in the restricted regions and that its relatively large amounts originated from soils. The North Han River showed a positive correlation of δ¹³C_{DIC} values with alkalinity, while the South Han River exhibited the opposite trend, indicating that the North Han River was likely affected by the DIC produced by the carbonate dissolution in the catchment area, and the South Han River—by the soil-derived DIC (Ryu et al., 2007).

The tributaries are distributed in the agricultural areas, and the soil organic matter mostly contributes to the DIC in the Nakdong River. Therefore, in the downstream regions, the oxidation of soil organic matter became more important in supplying DIC to the river water.

Statistical analysis

Table 2 reveals that the majority of ions have strong (0.60 ≤ |ρ| < 0.80) or very strong (0.80 ≤ |ρ| < 1.00) correlations with a high statistical significance with other ions except Si. In particular, Na⁺ shows significantly strong positive correlations with Cl and SO₄⁻ ions. The concentrations of those three ions, which were considered to originate from an anthropogenic source, abruptly increased at station 15, indicating that those three ions were mainly from the industrial complex in Daegu. However, NO₃⁻ ion, which was also considered to originate from an anthropogenic source, showed a relatively weak correlation with those three ions, indicating another source for this anion, probably from an agricultural source. With the exception of the relationship between δD and δ¹⁸O (ρ = 0.89), it is difficult to observe a distinctive relationship among δD, δ¹⁸O, δ¹³C_{DIC}, and ⁸⁷Sr/⁸⁶Sr in situ (i.e., EC and alkalinity) and in ion data (|ρ| < 0.5).

Principal component analysis (PCA) was applied to quantitatively evaluate the multivariate relation of the observed data. In this study, EC was not considered, and HCO₃⁻ was used instead of alkalinity for PCA. Table 3 gives the evaluated eigenvectors of three principal components (PC) corresponding to each data. Approximately 80% of the total data were conserved using three PCs. As seen in the table, the first PC (PC1) explains 45.63% of the total variance

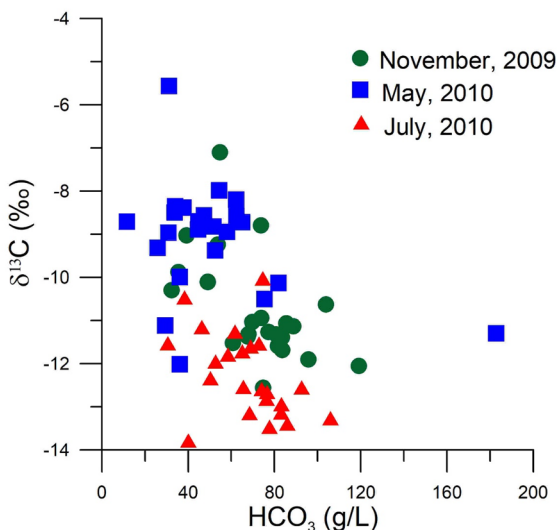


Fig. 10 Plots of δ¹³C_{DIC} versus alkalinity constructed for the water samples collected during different seasons

Table 2 Pearson correlation coefficients for the water chemistry data in this study

	EC	Alkalinity	K ⁺	Ca ²⁺	Mg ²⁺	Na ⁺	Si ⁺	HCO ₃ ⁻	Cl ⁻	NO ₃ ⁻	SO ₄ ²⁻	d ¹⁸ O	dD	d ¹³ C _{DIC}	⁸⁷ Sr/ ⁸⁶ Sr
EC	1.00														
Alkalinity	0.60***	1.00													
K ⁺	0.85***	0.59***	1.00												
Ca ²⁺	0.75***	0.73***	0.79***	1.00											
Mg ²⁺	0.81***	0.65***	0.87***	0.92***	1.00										
Na ⁺	0.89***	0.65***	0.94***	0.81***	0.86***	1.00									
Si ⁺	-0.04	0.08	-0.03	0.08	-0.02	-0.07	1.00								
HCO ₃ ⁻	0.60***	1.00***	0.59***	0.73***	0.65***	0.65***	0.08	1.00							
Cl ⁻	0.86***	0.65***	0.95***	0.80***	0.85***	0.97***	-0.09	0.65***	1.00						
NO ₃ ⁻	0.52***	0.37***	0.59***	0.57***	0.52***	0.65***	0.21*	0.37***	0.64***	1.00					
SO ₄ ²⁻	0.88***	0.53***	0.92***	0.81***	0.91***	0.93***	-0.13*	0.53***	0.92***	0.54***	1.00				
d ¹⁸ O	0.26**	0.25	0.35***	0.23*	0.37***	0.29***	-0.29*	0.25	0.38***	0.12	0.29***	1.00			
dD	0.13	0.10	0.24***	0.11	0.24*	0.23**	-0.28*	0.10	0.30***	0.13	0.19**	0.89***	1.00		
d ¹³ C _{DIC}	-0.27***	-0.46***	-0.24***	-0.31***	-0.22**	-0.21**	-0.52***	-0.46***	-0.22**	-0.22*	-0.08	-0.01	0.15	1.00	
⁸⁷ Sr/ ⁸⁶ Sr	-0.19	-0.15	-0.32***	-0.07	-0.16	-0.30**	-0.07	-0.16	-0.31***	-0.19	-0.17	-0.34***	-0.35***	0.33***	1.00

* Significant at 0.1 level; ** Significant at 0.05 level; *** Significant at 0.01 level

Table 3 Extracted eigenvectors corresponding to each data for three principal components (PC) based on the principal component analysis (PCA), and the percentage of the conserved information of each PC ($V_i, i = 1, \dots, 3$) to the total variance of the multivariate data, and its cumulative values

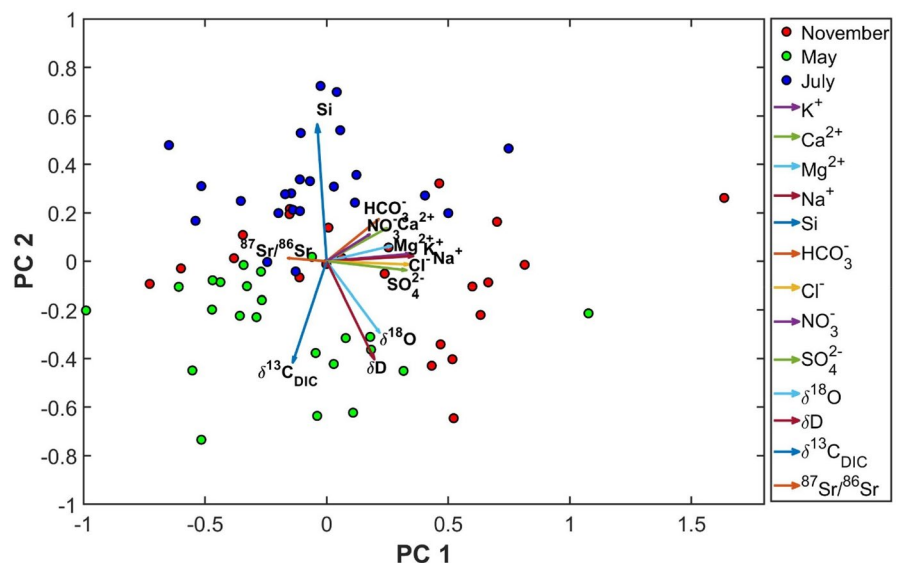
	PC1	PC2	PC3
K ⁺	0.3524	-0.0192	-0.0240
Ca ²⁺	0.2659	0.1270	0.1731
Mg ²⁺	0.2798	0.0420	0.1254
Na ⁺	0.3657	-0.0260	0.0613
Si ⁺	-0.0171	0.5891	-0.3985
HCO ₃ ⁻	0.2368	0.1769	0.1056
Cl ⁻	0.3378	-0.0683	-0.0296
NO ₃ ⁻	0.1780	0.0819	-0.0576
SO ₄ ²⁻	0.3401	-0.0751	0.2259
δ ¹⁸ O	0.1939	-0.3629	-0.2712
δ ² HD	0.1581	-0.4894	-0.3707
δ ¹³ C _{DIC}	-0.1615	-0.4158	0.3454
⁸⁷ Sr/ ⁸⁶ Sr	-0.1406	0.0759	0.6052
% of variance (V_i)	45.63	19.78	12.95
Cumulative V_i	45.63	65.41	78.36

of the data and is characterized by the positive loadings of K, Na, Cl, and SO₄, which are major ions from anthropogenic sources. This indicates that the Nakdong River is severely influenced by anthropogenic sources, especially from the industrial complex of Daegu, which is located downstream. The second PC (PC2) showed a positive loading for Si and negative

loadings for δD, δ¹⁸O, and δ¹³C_{DIC} with 19.78% of the total data. The components in the second PC are mainly controlled by weathering, and Si shows a negative correlation with δD, δ¹⁸O, and δ¹³C_{DIC}. Si in river water is supplied only by weathering of silicate minerals. The weathering of carbonate rocks with high δ¹³C_{DIC} decreases the relative concentration of Si in the river water, resulting in the negative correlation between Si and δ¹³C_{DIC}. The concentrations of Si were generally higher in July, in which the values of δD and δ¹⁸O were relatively low in the Nakdong River, causing the negative correlation of Si with δD and δ¹⁸O. The high Si concentrations in the flood season were also observed in The Yangtze River, which was interpreted to be related to the erodibility of parent rocks in the river basin during the monsoon precipitation (Li et al., 2007). In addition, ⁸⁷Sr/⁸⁶Sr, which did not show a noticeable correlation with other data, was evaluated as the third influential data that characterize the water chemistry of this river.

To visualize the relationship between the data, they were represented in two-dimensional data space reduced using the extracted PCs from the PCA (Table 3). Figure 11 presents the visualization result. In the figure, the x- and y-axis represent PC1 and PC2, respectively, and each circle corresponds to each data, with the different colored vectors indicating the direction of the variance of corresponding data. In addition, to evaluate the time-variant characteristics of the data, the data acquired at different

Fig. 11 The time-variant characteristics of the data distribution in the two-dimensional data space that reduced by using the PCA result



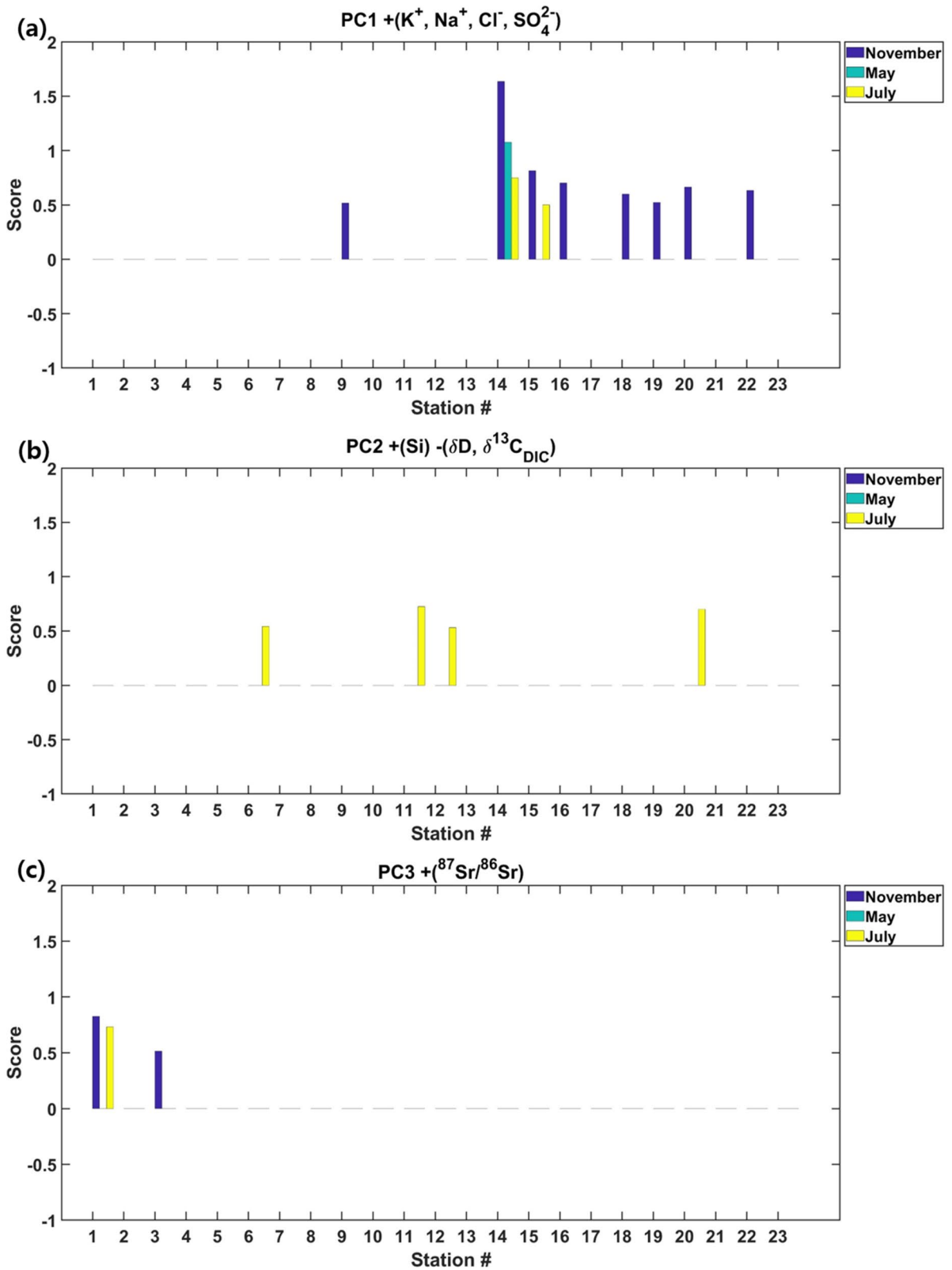


Fig. 12 The distribution of the scores of **a** PC1, **b** PC2, and **c** PC3 at each station for different sampling periods. The blue, green, and yellow bars indicate the score for November, May, and July, respectively

time periods were represented with circles of different colors (November: red circles; May: green circles; July: blue circles). As can be seen from the figure, the data acquired at the same period are close to each other and have an independent zone of dispersion in the data space. This means that the water chemistry of this river differs according to the sampling periods. In particular, November data (red circles) are distributed along the x-axis (PC1), which indicates that the concentration of PC1-related data (i.e., K, Na, Cl, and SO₄) tends to increase during November. Moreover, because the variance of blue circle data is high along the y-axis, it can be inferred that the Si concentration is likely to be high in July. However, the Si concentration conversely decreases in May, and δD, δ¹⁸O, and δ¹³C_{DIC} increase.

Figure 12 shows the value of the PC score at each station (from P1 to P23) for different sampling periods of November, May, and July with the blue, green, and yellow bars, respectively. In the figure, the height of each bar quantifies the impact on the water chemistry data corresponding to the evaluated PC. Only scores higher than 0.5 are presented; the results for PC1–PC3 are shown in Fig. 12. Overall, the influence on the water chemistry data for PC1 (K, Na, Cl, and SO₄) is relatively higher downstream of the river. In particular, station 14 (P14) shows the highest impact of PC1, and its influence is consistently high regardless of the sampling period, indicating that the data for PC1 are mainly influenced by the anthropogenic sources, especially in the downstream regions, including station 14. By contrast, as shown in Fig. 12c, the water chemistry upstream of the river is strongly influenced by weathering, which is represented by ⁸⁷Sr/⁸⁶Sr.

Conclusions

The results of this study showed that the concentrations of major ions and stable isotope values of the Nakdong River were influenced by both weathering and anthropogenic activities, including the industrial complex and agriculture. The stable isotope values of

δ¹³C_{DIC} and ⁸⁷Sr/⁸⁶Sr ratios provide useful information on the weathering process in the Nakdong River. In the upstream regions, weathering was the dominant process affecting the geochemistry of the rivers, which was also supported by the relatively high δ¹³C_{DIC} values, while Ca and HCO₃ were the main dissolved ions. In addition, the ⁸⁷Sr/⁸⁶Sr ratios indicate that upstream, the weathering of granite and gneiss complexes was significant, while downstream, the weathering of sedimentary rocks was more important. The concentrations of major ions and δ¹³C_{DIC} values also provide good information on the anthropogenic sources of contaminants. The concentrations of major ions gradually increased in downstream due to both weathering and agricultural activity, and after the inflow of the Kumho River, which was severely contaminated by the industrial complex and sewage treatment plant in Daegu, all ion concentrations (especially those of Na and SO₄ having anthropogenic origins) abruptly increased and gradually decreased again. These results suggest that the Nakdong River was mainly affected by the anthropogenic activities at the industrial complex and sewage treatment plant in Daegu. However, the obtained δ¹⁸O and δD values indicate that the effects of the water isotopes in the Kumho River were negligible. The δ¹³C_{DIC} values showed that in the downstream regions, its magnitudes depended on the oxidation of soil organic matter, which was enriched by the agricultural activity. The statistical analysis also demonstrates that anthropogenic sources, including industrial complex, have a significant influence on the water geochemistry (Na, Cl, and SO₄) in the downstream region, while weathering is the main factor affecting the river water chemistry in the upstream region. The geochemical characteristics of the Nakdong River significantly differed from those of the Han River, which was another major river in South Korea. Unlike the Han River, the chemical compositions in the Nakdong River were more strongly controlled by the anthropogenic activities.

Author contribution Conceptualization: K-SL, YK; methodology: GK, K-SL; formal analysis and investigation: GK, JJ; writing – original draft preparation: GK, YK; writing – review and editing: YK; funding acquisition: YK; supervision: YK.

Funding This study was supported by the Basic Science Research Program through the National Research Foundation of Korea (NRF) funded by the Korean government (MSIT) (No. 2016R1A2B1009477 and No. 2019R1A2C1002254).

Data availability All data generated or analyzed during this study are included in this published article.

Declarations

Ethics approval and consent to participate Not applicable.

Consent for publication Not applicable.

Competing interests Not applicable.

References

- Andrew, M. G., Jacobson, A. D., Lehn, G. O., Horton, T. W., & Craw, D. (2016). Radiogenic and stable Sr isotope ratios ($^{87}\text{Sr}/^{86}\text{Sr}$, $\delta^{88/86}\text{Sr}$) as tracers of riverine cation sources and biogeochemical cycling in the Milford Sound region of Fiordland, New Zealand. *Geochimica Cosmochimica Acta*, *173*, 284–303.
- Balagizi, C. M., Darchambeau, F., Bouillon, S., Yalire, M. M., Lambert, T., & Borges, A. V. (2015). River geochemistry, chemical weathering, and atmospheric CO_2 consumption rates in the Virunga Volcanic Province (East Africa). *Geochemistry, Geophysics, Geosystems*, *16*, 2637–2660.
- Barth, J. A. C., Cronin, A. A., Dunlop, J., & Kalin, R. M. (2003). Influence of carbonates on the riverine carbon cycle in an anthropogenically dominated catchment basin: Evidence from major elements and stable carbon isotopes in the Lagan River (N. Ireland). *Chemical Geology*, *200*, 203–216.
- Barth, J. A. C., & Veizer, J. (2004). Water mixing in a St. Lawrence river embayment to outline potential sources of pollution. *Applied Geochemistry*, *19*, 1637–1641.
- Bataille, C. P., & Bowen, G. J. (2012). Mapping Sr-87/Sr-86 variations in bedrock and water for large scale provenance studies. *Chemical Geology*, *304*, 39–52.
- Bataille, C. P., Brennan, S. R., Hartmann, J., Moosdorf, N., Wooller, M. J., & Bowen, G. J. (2014). A geostatistical framework to predict strontium isotopes variations in Alaska Rivers. *Chemical Geology*, *389*, 1–15.
- Bierman, P. B., Albrecht, A., Bothner, M. H., Brown, E. T., Bullen, T. D., Gray, L. B., & Turpin, L. (1998). Erosion, weathering, and sedimentation. In C. Kendall & J. J. McDonnell (Eds.), *Isotope Tracers in Catchment Hydrology* (pp. 647–678). Elsevier.
- Bishwakarma, K., Wang, G. -X., Zhang, F., Adhikari, S., Karki, K., & Ghimire, A. (2022). Hydrogeochemical characterization and irrigation suitability of the Ganges Brahmaputra River System: Review and assessment. *Journal of Mountain Science*, *19*, 388–402.
- Borg, L. E., & Banner, J. L. (1996). Neodymium and strontium isotopic constraints on soil sources in Barbados, West Indies. *Geochimica Et Cosmochimica Acta*, *60*, 4193–4206.
- Brennan, S. R., Fernandez, D. P., Mackey, G., Cerling, T. E., Bataille, C. P., Bowen, G. J., & Wooller, M. J. (2014). Strontium isotope variation and carbonate versus silicate weathering in rivers from across Alaska: Implications for provenance studies. *Chemical Geology*, *389*, 167–181.
- Brenot, A., Carignan, J., France-Lanord, C., & Benoît, M. (2007). Geological and land use control on $\delta^{34}\text{S}$ and $\delta^{18}\text{O}$ of river dissolved sulfate: The Moselle river basin, France. *Chemical Geology*, *244*, 25–41.
- Cai, Y., You, C. -F., Wu, S. -F., Cai, W. -J., & Guo, L. (2020). Seasonal variation in strontium and carbon isotope systematics in the Lower Mississippi River: Implications for chemical weathering. *Chemical Geology*, *553*, 119810.
- Chen, J., Wang, F., Xia, X., & Zhang, L. (2002). Major element chemistry of the Changjiang (Yangtze River). *Chemical Geology*, *187*, 231–255.
- Chop, J. W., Matsuda, M., Kawano, M., Wakimoto, T., & Min, B. Y. (1999). Contamination of PCBs in Nakdong River estuary, Korea. *Toxicological Environmental Chemistry*, *72*, 233–243.
- Chang, K. H. (1975). Cretaceous stratigraphy of Southeast Korea. *Journal of the Geological Society of Korea*, *11*, 1–23.
- Clark, I. D., & Fritz, P. (1997). *Environmental isotopes in Hydrogeology*. Lewis Publishers.
- Dellinger, M., Hilton, R. G., & Nowell, G. M. (2021). Fractionation of rhenium isotopes in the Mackenzie River basin during oxidative weathering. *Earth and Planetary Science Letters*, *573*, 117131.
- Dyrssen, D., & Sillén, L. G. (1967). Alkalinity and total carbonate in sea water. A plea for p-T-independent data. *Tellus*, *19*, 113–121.
- Edmond, J. M. (1970). High precision determination of titration alkalinity and total carbon dioxide content of sea water by potentiometric titration. *Deep Sea Research and Oceanographic Abstracts*, *17*, 737–750.
- Faure, G. (1977). *Principles of isotope geology*. John Wiley and Sons.
- Fricke, H. C., & O'Neil, J. R. (1999). The correlation between $^{18}\text{O}/^{16}\text{O}$ ratios of meteoric water and surface temperature: Its use in investigating terrestrial climate change over geologic time. *Earth and Planetary Science Letters*, *170*, 181–196.
- Gaillardet, J., Dupré, B., Louvat, P., & Allègre, C. J. (1999). Global silicate weathering and CO_2 consumption rates deduced from the chemistry of large rivers. *Chemical Geology*, *159*, 3–30.
- Galy, A., & France-Lanord, C. (1999). Weathering processes in the Ganges-Brahmaputra basin and the riverine alkalinity budget. *Chemical Geology*, *159*, 31–60.
- Gibbs, R. J. (1972). Water chemistry of the Amazon River. *Geochimica Et Cosmochimica Acta*, *36*, 1061–1066.
- Gordeev, V. V., & Sidorov, L. S. (1993). Concentrations of major elements and their outflow into the Laptev Sea by the Lena River. *Marine Chemistry*, *43*, 33–45.
- Hoefs, J. (2004). *Stable isotope geochemistry*. Springer.
- Holland, H. D. (1978). *The chemistry of the atmosphere and oceans*. Wiley.
- Huh, Y., Panteleyev, G., Babich, D., Zaitsev, A., & Edmond, J. M. (1998a). The fluvial geochemistry of the rivers of Eastern Siberia: II. Tributaries of the Lena, Omoloy, Yana, Indigirka/Kolyma, and Anadyr draining the collisional/accretionary zone of the Verkhoyansk and Cherskiy ranges. *Geochimica Et Cosmochimica Acta*, *62*, 2053–2075.
- Huh, Y., Tsoi, M. -Y., Zaitsev, A., & Edmond, J. M. (1998b). The fluvial geochemistry of the rivers of Eastern Siberia: I. Tributaries of the Lena River draining the sedimentary

- platform of the Siberian Craton. *Geochimica Et Cosmochimica Acta*, 62, 1657–1676.
- Kattan, Z. (2015). Chemical and isotopic characteristics of the Euphrates River water, Syria: Factors controlling its geochemistry. *Environmental Earth Sciences*, 73, 4763–4778.
- Kendall, C., & Coplen, T. B. (2001). Distribution of oxygen-18 and deuterium in river waters across the United States. *Hydrological Processes*, 15, 1363–1393.
- Kim, K., Hamm, S.-Y., Kim, R.-H., & Kim, H. (2018). A review on alkalinity analysis methods suitable for Korean groundwater. *Economic and Environmental Geology*, 51, 509–520.
- Kim, K. H., Heo, W. M., & Kim, B. (1998). Spatial and temporal variabilities in nitrogen and phosphorus in the Nakdong river system, Korea. *Water, Air, & Soil Pollution*, 102, 37–60.
- Kim, Y., & Kim, K. (2013). Hydrogeochemistry and isotopic study of the Kumho River, Korea: Implications for anthropogenic and seasonal effects. *Environmental Earth Sciences*, 68, 2051–2064.
- Kwon, J. H., Lee, H., Kwon, J. W., Kim, K., Park, E., Kang, M. H., & Kim, Y. H. (2008). Mutagenic activity of river water from a river near textile industrial complex in Korea. *Environmental Monitoring and Assessment*, 142, 289–296.
- Lamb, L. (2000). Correlation of conductivity and stable isotope ^{18}O for the assessment of water origin in river system. *Chemical Geology*, 164, 161–170.
- Lang, Y. C., Liu, C. Q., Li, S. L., Zhao, Z. Q., & Zhou, Z. H. (2011). Tracing natural and anthropogenic sources of dissolved sulfate in a karst region by using major ion chemistry and stable sulfur isotopes. *Applied Geochemistry*, 26, 5202–5205.
- Lee, K. S., Bong, Y. S., Lee, D., Kim, Y., & Kim, K. (2008). Tracing the sources of nitrate in the Han River watershed in Korea, using $\delta^{15}\text{N}\text{-NO}_3^-$ and $\delta^{18}\text{O}\text{-NO}_3^-$ values. *Science of the Total Environment*, 395, 117–124.
- Lee, K. S., & Chang, B. U. (1994). Oxygen and hydrogen isotopic composition of precipitation in Taejeon and Seoul, Korea. *Journal of the Geological Society of Korea*, 30, 475–481.
- Lee, K. S., Grundstein, A. J., Wenner, D. B., Choi, M. S., Woo, N. C., & Lee, D. H. (2003). Climate controls on the stable isotopic composition of precipitation in Northeast Asia. *Climate Research*, 23, 137–148.
- Lee, K. S., Ryu, J. S., Ahn, K. H., Chang, H. W., & Lee, D. (2007). Factors controlling carbon isotope ratios of dissolved inorganic carbon in two major tributaries of the Han River, Korea. *Hydrological Processes*, 21, 500–509.
- Li, X., Weng, B., Yan, D., Qin, T., Wang, K., Bi, W., Yu, Z., & Dorjsuren, B. (2019). Anthropogenic effects on hydrogen and oxygen isotopes of river water in cities. *International Journal of Environmental Research and Public Health*, 16, 4429.
- Li, X. D., Liu, C. Q., Liu, X. L., & Bao, L. R. (2011). Identification of dissolved sulfate sources and the role of sulfuric acid in carbonate weathering using dual-isotopic data from the Jialing River, Southwest China. *Journal of Asian Earth Sciences*, 42, 370–380.
- Li, C., Yan, S., Lian, E., Yang, C., Deng, K., & Liu, Z. (2016). Damming effect on the Changjian (Yangtze River) river water cycle based on stable hydrogen and oxygen isotopic records. *Journal of Geochem Exploration*, 165, 125–133.
- Li, M., Xu, K., Watanabe, M., & Chen, Z. (2007). Long-term variations in dissolved silicate, nitrogen, and phosphorus flux from the Yangtze River into the East China Sea and impacts on estuarine ecosystem. *Estuarine, Coastal and Shelf Science*, 71, 3–12.
- Li, S. -L., Liu, C. -Q., Lang, Y. -C., Tao, F., Zhao, Z., & Zhou, Z. (2008). Stable carbon isotope biogeochemistry and anthropogenic impact on Karst ground water, Zunyi, Southeast China. *Aquatic Geochemistry*, 14, 211–221.
- Marchina, C., Bianchini, G., Natali, C., Pennisi, M., Colombani, N., Tassinari, R., & Knoeller, K. (2015). The Po river water from the Alps to the Adriatic Sea (Italy): New insights from geochemical and isotopic ($\delta^{18}\text{O}\text{-}\delta\text{D}$) data. *Environmental Science and Pollution Research*, 22, 5184–5203.
- Négrel, P., Millot, R., Petelet-Giraud, E., & Klaver, G. (2020). Li and $\delta^7\text{Li}$ as proxies for weathering and anthropogenic activities: Application to the Dommel River (meuse basin). *Applied Geochemistry*, 120, 104674.
- Park, K. H., Lee, H. S., Song, Y. S., & Cheong, C. S. (2006). Sphene U-Pb ages of the granite-granodiorites from Hamyang, Geochang and Yeongju areas of the Yeongnam Massif. *Journal of the Petrological Society of Korea*, 15, 39–48.
- Quiñones, O., Oh, J. E., Vanderford, B., Kim, J. H., Cho, J., & Snyder, S. A. (2007). Perchlorate assessment of the Nakdong and Yeongsan watersheds, Republic of Korea. *Environmental Toxicology and Chemistry*, 26, 1349–1354.
- Revels, B. N., Rickli, J., Moura, C. A. V., & Vance, D. (2021a). Nickel and its isotopes in the Amazon Basin: The impact of the weathering regime and delivery to the ocean. *Geochimica Et Cosmochimica Acta*, 293, 344–364.
- Revels, B. N., Rickli, J., Moura, C. A. V., & Vance, D. (2021b). The riverine flux of molybdenum and its isotopes to the ocean: Weathering processes and dissolved-particulate partitioning in the Amazon basin. *Earth and Planetary Science Letters*, 559, 116773.
- Ryu, J. S., Lee, K. S., & Chang, H. W. (2007). Hydrogeochemical and isotopic investigations of the Han River basin, South Korea. *Journal of Hydrology*, 345, 50–60.
- Sarin, M. M., Krishnaswami, S., Dili, K., Somayajulu, B. L. K., & Moore, W. S. (1989). Major ion chemistry of the Ganga-Brahmaputra river system: Weathering processes and fluxes to the Bay of Bengal. *Geochimica Et Cosmochimica Acta*, 53, 997–1009.
- Stallard, R. F., & Edmond, J. M. (1981). Geochemistry of the Amazon: 1. Precipitation chemistry and the marine contribution to the dissolved load at the time of peak discharge. *Journal of Geophysical Research*, 86, 9844–9855.
- Stallard, R. F., & Edmond, J. M. (1983). Geochemistry of the Amazon: 2. The influence of geology and weathering environment on the dissolved load. *Journal of Geophysical Research*, 88, 9671–9688.
- Stallard, R. F., & Edmond, J. M. (1987). Geochemistry of the Amazon: 3. Weathering chemistry and limits to dissolved inputs. *Journal of Geophysical Research*, 92, 8293–8302.
- Vitória, L., Otero, N., Soler, A., & Canals, À. (2004). Fertilizer characterization: Isotopic data (N, S, O, C and Sr). *Environmental Science & Technology*, 38, 3254–3262.

- Wachniew, P. (2006). Isotopic composition of dissolved inorganic carbon in a large polluted river: The Vistula, Poland. *Chemical Geology*, *233*, 293–308.
- Winston, W. E., & Criss, R. E. (2003). Oxygen isotope and geochemical variations in the Missouri River. *Environmental Geology*, *43*, 546–556.
- Wu, Y., Luo, Z., Luo, W., Ma, T., & Wang, Y. (2018). Multiple isotope geochemistry and hydrochemical monitoring of karst water in a rapidly urbanized region. *Journal of Contaminant Hydrology*, *218*, 44–58.
- Xu, Z., Shi, C., Tang, Y., & Han, H. (2011). Chemical and strontium isotopic compositions of the Hanjing Rivers in China: Anthropogenic impacts and chemical weathering. *Aquatic Geochemistry*, *17*, 243–264.
- Zhang, J., Huang, W. W., Létolle, R., & Jusserand, C. (1995). Major element chemistry of the Huanghe (Yellow River), China – Weathering processes and chemical fluxes. *Journal of Hydrology*, *168*, 173–203.
- Zieliński, M., Dopieralska, J., Belka, Z., Walczak, A., Siepak, M., & Jakubowicz, M. (2017). The strontium isotope budget of the Warta River (Poland): Between silicate and carbonate weathering, and anthropogenic pressure. *Applied Geochemistry*, *81*, 1–11.
- Zieliński, M., Dopieralska, J., Królikowska-Ciągło, S., Walczak, A., & Belka, Z. (2021). Mapping of spatial variation in Sr isotope signatures ($^{87}\text{Sr}/^{86}\text{Sr}$) in Poland – Implication of anthropogenic Sr contamination for archaeological provenance and migration research. *Science of the Total Environment*, *775*, 145792.

Publisher's Note Springer Nature remains neutral with regard to jurisdictional claims in published maps and institutional affiliations.